

## Research Article

# Experimental Investigation of Decontamination Factor Dependence on Aerosol Concentration in Pool Scrubbing

Haomin Sun , Yasuteru Sibamoto, Yuria Okagaki, and Taisuke Yonomoto

Nuclear Safety Research Center, Japan Atomic Energy Agency, 2-4 Shirakata, Tokai-mura, Naka-gun, Ibaraki 319-1195, Japan

Correspondence should be addressed to Haomin Sun; [son.hiroaki@jaea.go.jp](mailto:son.hiroaki@jaea.go.jp)

Received 24 October 2018; Revised 30 April 2019; Accepted 14 May 2019; Published 10 June 2019

Academic Editor: Rafa Miró

Copyright © 2019 Haomin Sun et al. This is an open access article distributed under the Creative Commons Attribution License, which permits unrestricted use, distribution, and reproduction in any medium, provided the original work is properly cited.

Because a pool scrubbing is important for reducing radioactive aerosols to the environment for a nuclear reactor in a severe accident situation, many researches have been performed. However, decontamination factor (DF) dependence on aerosol concentration was seldom considered in an aerosol number concentration with limited aerosol coagulation. To investigate an existence of DF dependence on the concentration, DF in a pool scrubbing with 2.4 m water submergence was derived from aerosol measurements by light scattering aerosol spectrometers. It was observed that DF increased monotonically with decreasing particle number concentration in a constant thermohydraulic condition: a gradual increase from 10 to 32 in the range of  $1.3 \times 10^{11}$  -  $8.0 \times 10^{11}/\text{m}^3$  at the inlet and a significant increase from 32 to 77 in the range of  $3.6 \times 10^{10}$  -  $1.3 \times 10^{11}/\text{m}^3$ . Two validation experiments were conducted in the range with the gradual DF increase to confirm whether the DF dependence is a real pool scrubbing phenomenon. In addition, characteristics of the DF dependence in different water submergences were investigated experimentally. It was found that the DF dependence became more significant in higher water submergence. Significant DF dependence was observed in the condition of the water submergence higher than 1.6 m and the inlet particle number concentration less than around  $1 \times 10^{11}/\text{m}^3$ . It is recommended to perform further analysis for the DF dependence mainly in such condition since it could make a difference to both experiment and model of the pool scrubbing.

## 1. Introduction

During a severe accident of a nuclear reactor, fission products (FPs) may be released from degraded nuclear fuels. In addition to several preinstalled filters, pool scrubbing is a phenomenon to reduce FP release to the environment by retaining FPs into the liquid phase during gas flows with FPs passing through a pool of water. FPs can be in forms of gas and aerosol during their transportation. In this paper, we only focus on aerosol. Pool scrubbing is one of the most effective phenomena to filter out the aerosols with a relatively high aerosol removal efficiency, in other words a high decontamination factor (DF). It can occur in some components in nuclear power plants, such as a suppression pool in a boiling water reactor (BWR) when the aerosol laden gas is released there and a steam generator in a pressurized water reactor (PWR) when steam generator tube rupture (SGTR) occurs. In addition, regulatory requirement for filtered containment venting systems (FCVS) by the nuclear regulation authority in

Japan revised after the Fukushima-Daiichi accident increased the importance of pool scrubbing, which has common characteristics with phenomenon in FCVS. Because of the above-mentioned importance in a severe accident situation, many researches have been performed up to date.

Several pool scrubbing analysis codes such as SPARC [1], BUSCA [2], and SUPRA [3] have utilized fundamentally similar pool scrubbing models. In the models, a gas-liquid two-phase flow is divided into several zones depending on different hydrodynamic behaviors. A total DF is derived by multiplying DFs in each zone such as a gas injection zone and a bubble rise zone. In the bubble rise zone, a swam of bubbles is represented by a typical bubble whose characteristic parameters such as size, shape, and velocity are calculated from existing gas-liquid two-phase flow models. In this typical bubble, several aerosol removal models are considered. Kaneko et al. [4] proposed an empirical pool scrubbing model based on their experimental database. In

their pool scrubbing model, characteristics of a gas-liquid two-phase flow are not considered in detail.

On the other hand, many pool scrubbing experiments have been performed in 1980-1990s [5]. From their work, a general understanding of the pool scrubbing phenomenon can be achieved. To promote a better understanding of some specified phenomena and/or to obtain more accurate and qualified data by more sophisticated measuring techniques for improving the existing pool scrubbing models, several experiments were conducted as follows. Herranz et al. [6] performed a pool scrubbing experiment with a horizontal gas injection. DF in gas jet injection conditions was measured. Dehbi et al. [7] did an experiment in a low-subcooling pool under realistic accident conditions. It was pointed out that there was a large discrepancy of DF between the experiment and the analysis by BUSCA code. Recently, Uchida et al. [8] conducted a pool scrubbing experiment to understand a pool temperature effect on DF. In addition, Kanai et al. [9] constructed a database of DF in the bubble rise zone by an aerosol measurement instrument with a high particle size resolution.

In the existing pool scrubbing experiments, an experimental parameter of aerosol number concentration was seldom considered. It was probably because DF was assumed to be independent of aerosol number concentration, at least, in the concentration where an aerosol coagulation is limited. The existing pool scrubbing models also follow this assumption. To the best of our knowledge, there was only one experimental result showing DF dependence on aerosol concentration by Hashimoto et al. [10]. In their experiment, dioctyl phthalate (DOP) liquid aerosol was generated in the wide size range from 0.3 to 2  $\mu\text{m}$ . DFs in different inlet aerosol concentrations among  $10^{-3}$ -1 ppm were measured in constant thermohydraulic boundary conditions. Unfortunately, there was not any explanation; even no validation test was conducted to confirm this uncommon result.

Aerosol number concentration in a severe accident of a nuclear reactor is in the wide range depending on an accident scenario, elapsed time after the accident onset, location, particle characteristics, and so on. An aerosol mass concentration is usually considered to be less than  $1 \times 10^{-3}$   $\text{kg}/\text{m}^3$  in reactor accident analyses [11]. According to a FP test (FPT0) of PHEBUS which is aimed to investigate source term related phenomena in a representative condition of a severe accident, the aerosol mass concentration was lower than about  $6 \times 10^{-4}$   $\text{kg}/\text{m}^3$  in the containment with injecting aerosol generated from a degraded fuel [12]. Aerodynamic mean mass diameter of the aerosol was 1.3 - 3.5  $\mu\text{m}$  measured by an impactor. The aerosol number concentration in this test can be roughly estimated to be about  $5 \times 10^{10}$  -  $9 \times 10^{11}/\text{m}^3$  by assuming a monodisperse spherical particle with a density of  $1 \times 10^3$   $\text{kg}/\text{m}^3$ .

In this paper, a pool scrubbing experiment to investigate an existence of DF dependence on aerosol particle number concentration is presented. The result showed that DF increased monotonically as decreasing particle number concentration in a constant thermohydraulic condition: a gradual increase from 10 to 32 in the range of  $1.3 \times 10^{11}$

-  $8.0 \times 10^{11}/\text{m}^3$  at the inlet and a significant increase from 32 to 77 in the range of  $3.6 \times 10^{10}$  -  $1.3 \times 10^{11}/\text{m}^3$ . These aerosol number concentrations would not be a rare case in a severe accident condition based on the above-mentioned estimation. However, the DF dependence has been seldom accounted for in the existing pool scrubbing models and experiments for the nuclear reactor severe accident analysis. In order to confirm that the DF dependence is a real pool scrubbing phenomenon, several validation experiments were conducted. In addition, characteristics of the DF dependence were investigated experimentally and mechanisms for the DF dependence were discussed.

## 2. Experimental System

*2.1. Experimental Apparatus.* A schematic diagram of a pool scrubbing test apparatus named PONTUS (pool scrubbing test unit on separate effect) is presented in Figure 1. The test section was constructed by connecting polycarbonate pipes with each other. An inner diameter of the pipes is 0.2 m and lengths range from 0.3 to 1 m. The maximum length of the test section was about 4.5 m. An aerosol laden air flow was injected upwardly into the test section from its bottom through a straight bore nozzle with an inner diameter of  $10 \times 10^{-3}$  m. In the pool scrubbing experiment, the test section was filled with deionized water. After the air flow passing through the test section and an outlet aerosol sampling pipe, it was exhausted to the environment through a flexible duct with an inner diameter and a length of about 0.2 m and 10 m, respectively. There is not any filter installed at the exit of the duct in order to maintain the test section in the atmospheric pressure condition. Several K-type thermocouples were installed to measure temperatures of air and water. A pressure transmitter (AP-52A, KEYENCE Corp.,  $\pm 0.5\%$  F.S. of 100 kPa) was applied to the same height of the air injection nozzle exit to measure the hydrostatic pressure there. The atmospheric pressure was measured by a barometer.

Aerosol was generated by an aerosol generation system (RBG, PALAS Corp.). In this system, solid particles in a container were supplied to a rotating brush by a moving piston and dispersed by a particle free air. Aerosol particle number concentration can be increased by increasing the moving piston velocity and by installing the container with a larger cross-section. Particle diameter distribution changed little by these operations in our experiments. The flow rate of this particle dispersing air was controlled by a mass flow controller (MQV0200, AZBIL Corp.,  $\pm 1\%$  F.S. of  $3.3 \times 10^{-3}$   $\text{m}^3/\text{s}$  in 293 K and 101 kPa). In the downstream of the aerosol generation system, a neutralizer (EAN 581, TOPAS Corp.) was installed to electrically neutralize charged particles by providing another particle free air flow with high bipolar ion concentration to the aerosol laden flow. Undesired electrical effects on particles can be reduced as much as possible by this neutralizer with setting its maximum ionization current of  $\pm 50$   $\mu\text{A}$ . The flow rate of this discharging air was controlled by a mass flow controller (HFC-303, KOFLOC Corp.,  $\pm 1\%$  F.S. of  $5.0 \times 10^{-3}$   $\text{m}^3/\text{s}$  in 293 K and 101 kPa). The total air flow

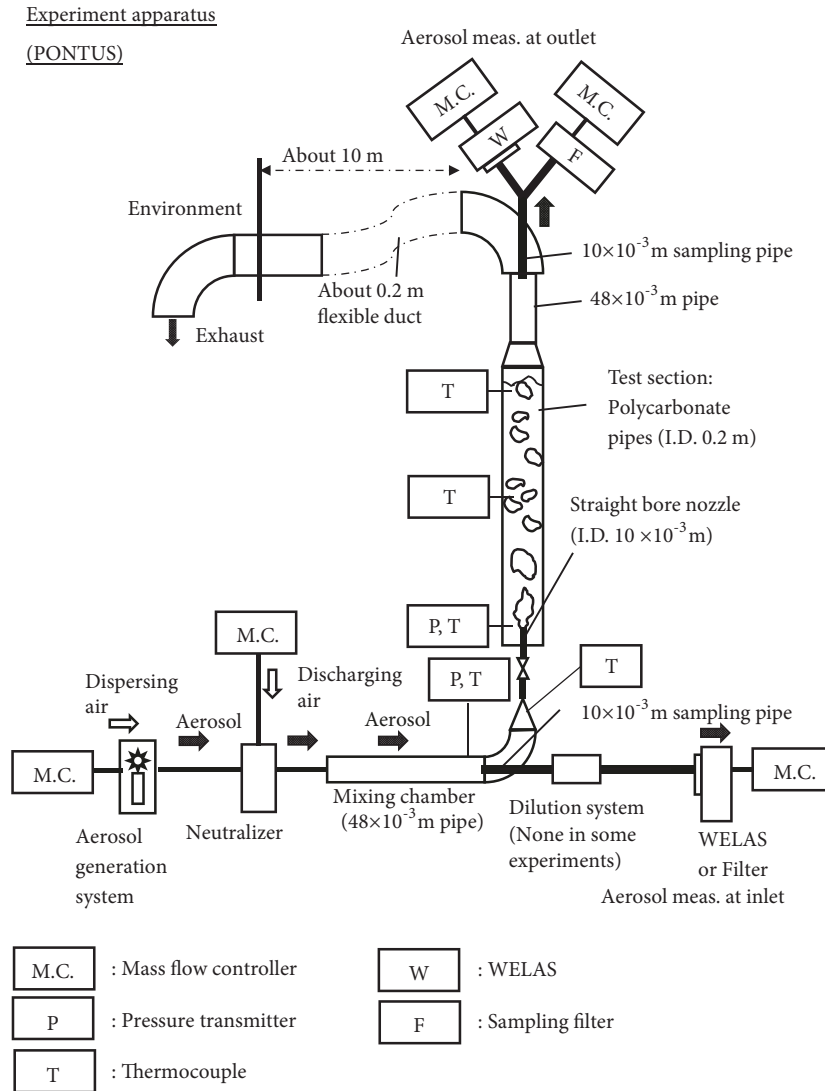


FIGURE 1: Schematic diagram of experimental apparatus.

rate after this neutralizer to a mixing chamber is a sum of the dispersing air flow from the aerosol generation system and the discharging air flow from the neutralizer.

**2.2. Aerosol Measurement System.** In our experiment, aerosols at the inlet and outlet of the test section were sampled through  $10 \times 10^{-3}$  m sampling pipes located at the center of aerosol transportation pipes with the same inner diameter of  $48 \times 10^{-3}$  m as shown in Figure 1. Aerosols to each aerosol measurement instrument were aspirated by vacuum pumps and their gas flow rates were controlled by mass flow controllers, respectively. Aerosol measurement can be conducted by light scattering aerosol spectrometers (WELAS, PALAS Corp.) and sampling glass fiber filters. Instrument installation depends on each experiment and will be described later in detail.

Particle number and number concentration distributions in the particle diameter ranging from 0.27 to 10  $\mu\text{m}$  were measured by WELAS. Here, the concentration is in the

sampling gas pressure and temperature condition where the WELAS sensor locates. Before an experiment, WELAS was always calibrated by a type of standard particles with a particle diameter of about 1  $\mu\text{m}$ . The sampling flow rate of WELAS was controlled to  $8.3 \times 10^{-5}$  m<sup>3</sup>/s in the condition of 293 K and 101 kPa by a mass flow controller (MQV0020, AZBIL Corp.,  $\pm 0.5\%$  F.S. of  $3.33 \times 10^{-4}$  m<sup>3</sup>/s in 293 K and 101 kPa). There are three advantages of WELAS for our experiment. First, aerosol measurement can be performed by WELAS directly at the inlet without reducing the hydrostatic pressure by a valve or an orifice where undesired particle loss may occur. Second, since WELAS is an in-line measurement device, it allows us to adjust the aerosol generation system for setting aerosol particle number concentration easily and monitor the concentration change after the adjustment. Third, WELAS has a high resolution of particle diameter in the diameter range of our test particle. On the other hand, there are two disadvantages. First, particle diameter measured by WELAS is a light scattering based diameter but not an

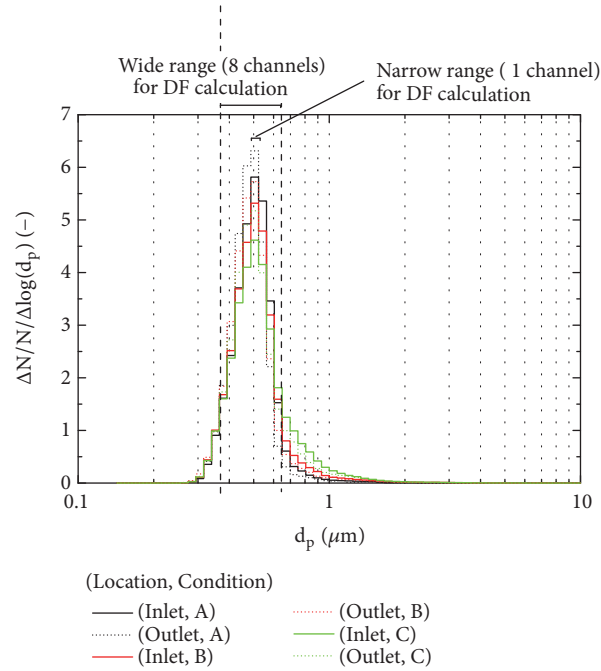


FIGURE 2: Particle diameter distributions of test particle measured by WELAS.

aerodynamic diameter which is often used for considering particle motion. In order to make relationship between these two diameters, white spherical particles were adopted. Second, a coincidence error due to multiparticles in its sensing volume simultaneously will be increased significantly as increasing particle number concentration beyond a certain number concentration. To perform a reliable measurement, measurement accuracy of WELAS was considered in advance based on an experimental comparison between WELAS and a condensation particle counter (CPC 3776, TSI Corp.) for our test particle [13]. It was confirmed that difference of aerosol number concentration measured by WELAS and CPC was  $\pm 10\%$  in the range from  $4.0 \times 10^9$  to  $1.2 \times 10^{11}/\text{m}^3$ . Therefore, almost all the WELAS measurements were conducted in the concentration less than  $1.2 \times 10^{11}/\text{m}^3$  to avoid the coincidence error. To reduce aerosol number concentration, a dilution system (VKL 10E, PALAS Corp.) was always installed in the upstream of WELAS at the inlet of the test section only in a pool scrubbing experiment. No dilution system was done for WELAS at the outlet. All the gas flow rates of this dilution system were controlled to  $7.5 \times 10^{-4} \text{ m}^3/\text{s}$  in the condition of 293 K and 101 kPa by mass flow controllers (MQV0050, AZBIL Corp.,  $\pm 1.5\%$  F.S. of  $8.3 \times 10^{-4} \text{ m}^3/\text{s}$  in 293 K and 101 kPa), respectively.

On the other hand, aerosol can be sampled by a sampling glass fiber filter for aerosol measurement. The sampling flow rate of the sampling filter was controlled to  $3.3 \times 10^{-4} \text{ m}^3/\text{s}$  in the condition of 293 K and 101 kPa by a mass flow controller (MQV0050, AZBIL Corp.,  $\pm 0.5\%$  F.S. of  $8.3 \times 10^{-4} \text{ m}^3/\text{s}$  in 293 K and 101 kPa). The filter before and after sampling aerosols was weighed by a microbalance (XPR2UV, Mettler Toledo Corp., Error  $< 1\%$  for weight  $> 2.1 \times 10^{-8} \text{ kg}$ ) to evaluate a total weight of sampled particle. In advance to measure the weight,

the filter was heated by an oven to reduce an undesired effect of humidity. In general, a sampling filter measurement is more reliable due to its simple principle. In addition, since it is also not necessary to install a valve or an orifice and a dilution system in its upstream, errors from these devices can be avoided. However, particle diameter and particle number concentration are not available by the sampling filter. In this study, the sampling filter was used to confirm DF derived from WELAS measurements.

In all the experiments, a type of white insoluble and hydrophilic  $\text{SiO}_2$  particles with a spherical shape was adopted as test particles. The density of  $\text{SiO}_2$  is  $2.2 \times 10^3 \text{ kg}/\text{m}^3$ . An example of measured particle diameter distributions by WELAS for the aerosol from this test particle was presented in Figure 2. Here,  $N$  and  $d_p$  are total particle number and particle diameter, respectively. The mode diameter and the geometric standard deviation were  $0.5 \mu\text{m}$  and 1.2 - 1.3, respectively. Based on the geometric standard deviation, the aerosol can be regarded as monodisperse.

### 3. DF Evaluation

In this study, DF was derived from measurement results by two different WELAS sensors or two different sampling filters. DF from WELAS measurement was evaluated as

$$DF = \frac{N_{t,in}}{N_{t,out}}. \quad (1)$$

Here,  $N_{t,in}$  and  $N_{t,out}$  are aerosol particle numbers of the aerosols in and out the test section, respectively, in the same particle diameter range and the same measurement time. Since Stokes numbers at the inlets of both sampling pipes were less than  $3 \times 10^{-4}$  in all the experiments, a sampling

error due to a superisokinetic sampling can be ignored [14]. Consequently,  $N_{t,in}$  and  $N_{t,out}$  can be given as

$$N_{t,in} = N_{s,in} \frac{W_{t,in}}{W_{s,in}} \quad (2)$$

$$N_{t,out} = N_{s,out} \frac{W_{t,out}}{W_{s,out}}. \quad (3)$$

Here,  $N_{s,in}$  and  $N_{s,out}$  are particle numbers of the aerosols sampled at the inlet and outlet, respectively.  $W_{t,in}$  and  $W_{t,out}$  are mass flow rates of the air flow in and out the test section, respectively.  $W_{s,in}$  and  $W_{s,out}$  are mass flow rates of the sampling air at the inlet and outlet, respectively. Since  $W_{s,in}$  and  $W_{s,out}$  were controlled to be the same mass flow rate (equivalent to  $8.3 \times 10^{-5} \text{ m}^3/\text{s}$  in 293 K and 101 kPa) and  $W_{t,in} = W_{t,out}$ , DF can be derived from measurement results of WELAS as

$$DF = \frac{N_{s,in}}{N_{s,out}} = \frac{D \cdot N_{w,in}}{N_{w,out}}. \quad (4)$$

Here,  $N_{w,in}$  and  $N_{w,out}$  are particle numbers of the aerosols measured by two different WELAS sensors at the inlet and outlet of the test section, respectively, in the same particle diameter range and the same measurement time.  $D$  is a dilution rate of the dilution system. In all the pool scrubbing experiments, the dilution system was always installed for WELAS measurement at the inlet only but not at the outlet. In the experiments with an empty test section, no dilution system was applied. The dilution rate was experimentally calibrated to be 8.7 for our test particles in advance. For the calibration procedure, refer to [15]. It is worth noting that relative values of DF in the same pool scrubbing experiments will not be affected by the error of this dilution rate since the same dilution system was always installed at the inlet and this constant dilution rate was always substituted to (4).

On the other hand, DF from two different sampling filters was evaluated as

$$DF = \frac{M_{t,in}}{M_{t,out}}. \quad (5)$$

Here,  $M_{t,in}$  and  $M_{t,out}$  are total particle weights of the aerosols in and out the test section in the same measurement time, respectively. In the sampling filter measurement,  $W_{s,in}$  and  $W_{s,out}$  were controlled to be the same mass flow rate (equivalent to  $3.3 \times 10^{-4} \text{ m}^3/\text{s}$  in 293 K and 101 kPa). Similar to DF from WELAS measurements described above, DF from the sampling filter measurements can be calculated as

$$DF = \frac{M_{f,in}}{M_{f,out}}. \quad (6)$$

Here,  $M_{f,in}$  and  $M_{f,out}$  are total particle weights of the aerosols sampled by the filters at the inlet and outlet, respectively. No dilution system was applied for the sampling filter.

Particle loss between the water surface and the top of the test section may also affect a value of DF, although this effect is limited [15]. To avoid this undesired effect, a distance between those was set to be shorter than 0.55 m by arranging the polycarbonate pipes for each water submergence.

#### 4. Experiment of DF Dependence on Aerosol Concentration

A pool scrubbing experiment (PW1) was performed to investigate DF in a constant thermohydraulic condition with different aerosol particle number concentrations. Experimental conditions and aerosol related descriptions of all the experiments in this paper including this experiment (PW1) are summarized in Table 1. Two different WELAS sensors were installed at the inlet and outlet of the test section, respectively. The dilution system was applied for WELAS sensor at the inlet of the test section but none was at the outlet. At the outlet, water droplets may be generated. In order to avoid miscounting of the droplets by WELAS at the outlet, WELAS sensor there was heated up to 393 K. Accordingly, WELAS sensor at the inlet was also heated to the same temperature for having the same measurement condition. In this temperature, only the droplets can be evaporated but not the test particle.

The water submergence was 2.4 m. The volumetric air flow rate at the exit of the injection nozzle was set to be  $1.3 \times 10^{-3} \text{ m}^3/\text{s}$  in the air temperature and pressure conditions there. Detailed flow rates of the dispersing air and the discharging air in the condition of 293 K and 101 kPa are also presented in Table 1. Temperatures of air and water were  $282 \pm 3 \text{ K}$ .

Detailed information of aerosol measurement in this experiment is presented in Table 2. In the constant thermohydraulic condition, the experiment started from the lowest particle number concentration and the concentration was increased by adjusting the aerosol generation system: increasing the piston moving velocity and setting the container of particles with a larger cross-section. After each adjustment for setting a new particle number concentration condition, a waiting time was provided for allowing aerosol to be transported to the outlet of the test section before aerosol measurements for DF. During each waiting time, particle number concentration changes at the inlet and outlet were monitored by two different WELAS sensors. The recorded monitoring time was longer in lower concentration condition and in the range of 300 - 600 s. Although each waiting time was not recorded specifically, it must be longer than the monitoring time. After reaching a steady-state condition, aerosol particle number distributions in particle diameter at the inlet and outlet were measured by two different WELAS sensors simultaneously for obtaining DF. In each particle number concentration condition, WELAS measurements in a measurement time were repeated usually more than 3 times. A value of DF was obtained in each measurement based on (4) with the dilution rate of 8.7. In order to measure enough particles statistically, the measurement time was longer in lower particle number concentration and in the range of 300 - 600 s. More than  $3 \times 10^3$  particles were measured in each measurement.

Particle diameter distributions measured by WELAS at the inlet and outlet in the lowest and highest particle number concentration conditions and in between were presented in Figure 2. The concentration conditions (A - C) are indicated in Figure 3. Their distributions were almost the same with

TABLE 1: Experimental conditions and aerosol related descriptions of all the experiments.

Experiment	Dispersing flow rate <sup>(a)</sup> (m <sup>3</sup> /s)	Discharging flow rate <sup>(a)</sup> (m <sup>3</sup> /s)	Injection flow rate <sup>(a,b)</sup> (m <sup>3</sup> /s)	Atmospheric pressure (kPa)	Hydrostatic pressure at nozzle exit (kPa)	Air and water temperatures (K)	Injection flow rate <sup>(c)</sup> at nozzle exit (m <sup>3</sup> /s)	Submergence (m)	Instruments for DF	Other instruments	Mode diameter <sup>(d)</sup> (μm)
PW1	$6 \times 10^{-4}$	$1.2 \times 10^{-3}$	$1.7 \times 10^{-3}$	102	21	$282 \pm 3$		2.4	WELAS sensors	Dilution (Inlet)	
PW2	$6 \times 10^{-4}$	$1.1 \times 10^{-3}$	$1.6 \times 10^{-3}$	101	15	$283 \pm 3$		1.6	WELAS sensors	Dilution (Inlet)	
PW3	$5 \times 10^{-4}$	$1.1 \times 10^{-3}$	$1.5 \times 10^{-3}$	102	7	$287 \pm 4$		0.8	WELAS sensors	Dilution (Inlet)	
PW4	$5 \times 10^{-4}$	$1.0 \times 10^{-3}$	$1.4 \times 10^{-3}$	101	2	$281 \pm 4$	$1.3 \times 10^{-3}$	0.3	WELAS sensors	Dilution (Inlet)	0.5
PF1	$7 \times 10^{-4}$	$1.4 \times 10^{-3}$	$1.7 \times 10^{-3}$	101	21	$283 \pm 3$		2.4	Filters	WELAS sensor (Outlet)	
PF2	$7 \times 10^{-4}$	$1.4 \times 10^{-3}$	$1.7 \times 10^{-3}$	101	21	$284 \pm 4$		2.4	Filters	WELAS sensor (Outlet)	
EW1	$5 \times 10^{-4}$	$1.0 \times 10^{-3}$	$1.3 \times 10^{-3}$	100	0	$293 \pm 2$		0	WELAS sensors	None	

<sup>(a)</sup> In the condition of 293 K and 101 kPa.

<sup>(b)</sup> A sum of dispersion and discharging flow rates minus inlet sampling flow rate.

<sup>(c)</sup> In the condition of actual gas temperature and pressure at injection nozzle exit.

<sup>(d)</sup> Measured by WELAS.

TABLE 2: Aerosol measurement information of the experiment PW1.

Averaged number concentration at outlet* ( $1/m^3$ )	Monitoring time (s)	Measurement time (s)	Number of measurements (-)
$4.9 \times 10^8$	600	600	4
$5.3 \times 10^8$	600	300	2
$1.1 \times 10^9$	300	300	4
$4.4 \times 10^9$	300	300	6
$9.1 \times 10^9$	300	300	5
$1.6 \times 10^{10}$	300	300	4
$3.7 \times 10^{10}$	300	300	3
$5.6 \times 10^{10}$	300	300	4
$8.2 \times 10^{10}$	300	300	4

\*Condition was set in the order from the top.

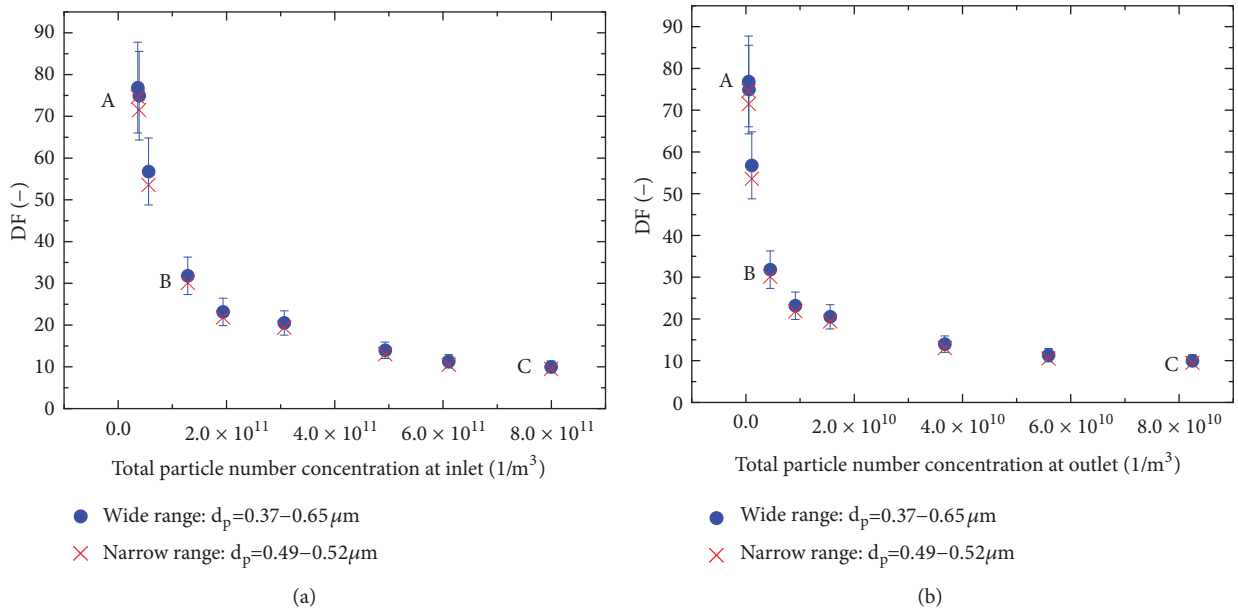


FIGURE 3: DF derived from WELAS against total particle number concentration (a) at inlet and (b) at outlet.

mode diameters of  $0.5 \mu\text{m}$  and geometric standard deviations of 1.2 - 1.3 because the aerosol was monodisperse. DFs and total particle number concentrations at the inlet and outlet obtained in each particle number concentration condition, in other words each setting of the aerosol generation system, were averaged by number of measurement ( $n$ ) based on (7)–(9), respectively, since they were in the same steady-state condition.

$$DF = \frac{\sum_i DF_i}{n} \quad (7)$$

$$C_{in} = \frac{\sum_i C_{in,i}}{n} \quad (8)$$

$$C_{out} = \frac{\sum_i C_{out,i}}{n}. \quad (9)$$

Here,  $DF_i$ ,  $C_{in,i}$ , and  $C_{out,i}$  are DF, the inlet, and outlet total particle number concentrations obtained in  $i$ -th aerosol

measurement in each condition.  $DF$ ,  $C_{in}$ , and  $C_{out}$  are the averaged DF, the averaged inlet, and outlet total particle number concentrations, respectively. The averaged DFs against the averaged total particle number concentrations at the inlet and the outlet were plotted in Figures 3(a) and 3(b), respectively. Here, the presented concentration at the inlet was the concentration before dilution by multiplying the dilution rate of 8.7 to the measured concentration. In addition, it was converted to the concentration in the atmospheric pressure condition by taking the measured hydrostatic pressure into consideration. In Figure 3, two different types of DF were plotted in each concentration condition. They were calculated based on the particle number ratio in a narrow and a wide particle diameter ranges, respectively, from the same aerosol measurement raw data. These two particle diameter ranges were shown in Figure 2. One was in the range of  $0.37 - 0.65 \mu\text{m}$  (8 particle diameter channels for WELAS) and the other was in the range of  $0.49 - 0.52 \mu\text{m}$  (single particle diameter

channel for WELAS). They were partially interrupted. As presented in Figure 3, both averaged DFs were almost the same because the aerosol was monodisperse. Since a value of DF based on a single particle diameter channel may be sensitive to the particle size calibration of WELAS, all the DFs by WELAS measurement will be evaluated based on the particle numbers in the above-mentioned wide range (0.37-0.65  $\mu\text{m}$ ) in this paper. As shown in Figure 3, DF increased monotonically with decreasing aerosol particle number concentration: a gradual increase from 10 to 32 in the range of  $1.3 \times 10^{11}$  -  $8.0 \times 10^{11}/\text{m}^3$  at the inlet and a significant increase from 32 to 77 in the range of  $3.6 \times 10^{10}$  -  $1.3 \times 10^{11}/\text{m}^3$ . The tendency of the DF dependence was similar to that measured by Hashimoto et al. [10].

In general, DF in the pool scrubbing depends on the hydrodynamics in the pool. Although we mainly focused on aerosol measurements for DF but not the hydrodynamics and detailed gas-liquid two-phase flow measurement was not performed in this study, some approximate explanations about the hydrodynamics in this experiment are made below based on the flow observation and the measured two-phase hydrostatic pressure  $P_t$ . It was observed that initial large bubbles were generated intermittently at the exit of the injection nozzle. A swarm of bubbles covering the whole cross-section of the test section was formed in the downstream of the initial bubble. In the swarm, relatively large bubbles with higher rising velocities were observed intermittently. A gas superficial velocity  $J_g$  close to the water surface was 0.052 m/s. A flow regime map for a bubble column depending on the column diameter  $D_c$  and  $J_g$  has been proposed [16]. It was also pointed out that a flow transition from the bubbly flow to the churn-turbulent flow will occur in a lower gas superficial velocity by orifices with diameters larger than 1 mm compared to a porous sparger with much smaller pores. Taking the flow observation and the flow regime map into consideration, the two-phase flow in the swarm region will be the churn-turbulent flow or a flow during transition but not the bubbly flow. The measured two-phase hydrostatic pressure  $P_t$  was 21 kPa in this experiment. The hydrostatic pressure  $P_l (= \rho_l g H)$  in a 2.4 m water submergence with liquid single-phase is 23.5 kPa in the water temperature of 282 K. Here,  $\rho_l$ ,  $g$ , and  $H$  are water density, acceleration of gravity ( $9.8 \text{ m/s}^2$ ), and a pool height, respectively. According to these hydrostatic pressures, the volumetric void fraction  $\alpha_v (= (P_l - P_t)/P_l)$  in the two-phase flow is calculated to be 0.11. Assuming that  $\alpha_s \cong \alpha_v$ , the cross-sectional averaged bubble rising velocity  $U_b$  in the downstream especially close to the water surface can be roughly estimated to be 0.5 m/s by taking  $U_b = J_g/\alpha_s$  into consideration. Here,  $\alpha_s$  is a cross-sectional averaged void fraction there. It is worth noting that the local bubble rising velocity in the center of the test section is expected to be higher than  $U_b$  due to a high bubble concentration there. On the other hand, that near the test section wall will be lower than  $U_b$  or even be minus due to a water circulation. A correlation of the bubble Sauter mean diameter  $D_{sm}$  in bubble columns has been proposed [17] as

$$D_{sm} = 26D_c \left( \frac{gD_c^2 \rho_l}{\sigma} \right)^{-0.5} \left( \frac{gD_c^3}{\nu_l^2} \right)^{-0.12} \left( \frac{J_g}{\sqrt{gD_c}} \right)^{-0.12} \quad (10)$$

Here,  $\sigma$  and  $\nu_l$  are surface tension and water kinematic viscosity, respectively. It was indicated that this correlation was applicable for a bubble column with a diameter up to 0.6 m, a gas superficial velocity up to 0.42 m/s, and a void fraction up to 0.3. Based on this correlation, the bubble Sauter mean diameter in this experiment is estimated to be  $6 \times 10^{-3}$  m.

In order to make sure that this DF dependence was not due to our experimental system error including measuring instrument and was a real pool scrubbing phenomenon, two validation experiments were performed.

## 5. Validation Experiments

**5.1. DF Derived from Sampling Filter.** In order to make sure that the DF dependence was not due to a measurement error of WELAS, two experiments (PF1 and PF2 in Table 1) were performed in other days to derive DF based on aerosol measurements by two sampling filters installed at the inlet and outlet. Here, PF2 was a repeating experiment for PF1 performed in the other day. The experimental conditions were summarized in Table 1. In these experiments, two sampling filters were installed at the inlet and outlet of the test section, respectively, without any dilution system. In addition, a WELAS sensor heated to 393 K was set at the outlet only without any dilution system.

The water submergence and the volumetric air flow rate at the exit of the injection nozzle were the same as those in the previous experiment (PW1), respectively. The temperatures of air and water were also almost the same as those in the previous experiment (PW1). DF in these experiments was derived from a measurement by the filters but not by WELAS. The purpose of measurement by WELAS at the outlet was to obtain particle number concentration distribution which is not available by the filter and to compare DF from the filters in these experiments with that from WELAS in the previous one.

Detailed information of aerosol measurement in these experiments is presented in Table 3. The experimental procedure was similar to the experiment PW1 except for the order of setting aerosol particle number concentration. In the above-mentioned constant thermohydraulic condition, the number concentration was changed (not increased monotonically from the lowest concentration) by adjusting the aerosol generation system in the same way. This was to make sure that the DF dependence did not result from an order of setting the number concentration. After each adjustment, a waiting time more than 300 s was provided. In each number concentration condition, aerosol measurements by a WELAS sensor at the outlet and two sampling filters were performed once and simultaneously with the same measurement time. Since the aerosol concentration at the inlet was always higher than that at the outlet, the sampled total particle weight at the inlet was always heavier than that at the outlet. The measurement time in each measurement was designed to sample particles

TABLE 3: Aerosol measurement information of the experiments PF1 and PF2.

Experiment	Averaged number concentration at outlet* (1/m <sup>3</sup> )	Waiting time (s)	Measurement time (s)	Number of measurements (-)
PF1	2.1×10 <sup>10</sup>	300**	1800	1
	3.6×10 <sup>10</sup>		900	
	6.5×10 <sup>10</sup>		510	
	1.0×10 <sup>11</sup>		360	
	3.6×10 <sup>9</sup>		11100	
PF2	7.7×10 <sup>9</sup>	300**	4530	1
	3.4×10 <sup>10</sup>		960	
	1.1×10 <sup>11</sup>		300	
	7.8×10 <sup>10</sup>		420	

\*Condition was set in the order from the top.

\*\*Longer than this as an experimental protocol but no specific data for each condition.

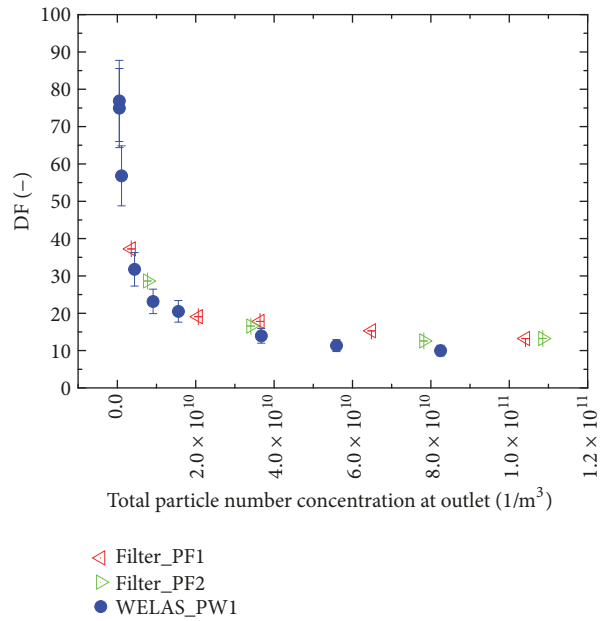


FIGURE 4: Comparison of DFs derived from filter and WELAS.

by the filter at the outlet with the total weight close to  $2 \times 10^{-6}$  kg taking measurement error of the microbalance into consideration. Here, the total particle weight sampled by the filter was estimated by the particle number concentration monitored by the WELAS sensor at the outlet during the measurement and by assuming a spherical particle with a particle diameter and a density of  $0.5 \mu\text{m}$  and  $2.2 \times 10^3 \text{ kg/m}^3$ , respectively. As a result, the measurement time in all the measurements was in the range of 300-11100 s and the total particle weight at the outlet was in the range of  $1.6 \times 10^{-6}$  -  $2.2 \times 10^{-6}$  kg. A value of DF was calculated from a ratio of total particle weight of the sampling filters at the inlet and outlet based on (6).

In these experiments, the mode diameter measured by WELAS at the outlet was  $0.5 \mu\text{m}$  in all the total particle number concentrations. DFs derived from the sampling filters were plotted in Figure 4 against total particle number

concentrations at the outlet. Since the aerosol measurement by WELAS was only conducted at the outlet but not at the inlet, DF against total particle number concentration at the inlet was not available in these experiments. For comparison, DF derived from WELAS in Figure 3(b) was also presented in Figure 4. In the outlet particle number concentration higher than  $3.6 \times 10^9 / \text{m}^3$ , DF by the sampling filters showed the same tendency as that by WELAS and they agreed well, especially in low aerosol concentrations, which strongly supported that the DF dependence in this concentration range was not due to an aerosol measurement error. It is worth noting that the DF dependence was not because of an error of the dilution system, since it was not applied in these experiments. Unfortunately, none of DF from the sampling filters was available in the concentration less than  $1.1 \times 10^9 / \text{m}^3$  where DF from WELAS was higher than 57. This is because a measurement time is estimated to be too long (about 36000

TABLE 4: Aerosol measurement information of the experiment EW1.

Averaged number concentration at outlet* ( $1/m^3$ )	Monitoring time (s)	Measurement time (s)	Number of measurements (-)
$5.3 \times 10^9$	900	600	4
$7.7 \times 10^9$	600	600	3
$1.4 \times 10^{10}$	600	300	4
$2.5 \times 10^{10}$	600	300	4
$5.1 \times 10^{10}$	300	300	2
$1.2 \times 10^{11}$	600	100	3
$6.6 \times 10^{10}$	300	160	3

\*Condition was set in the order from the top.

s) to perform a measurement in this concentration with a sampled total particle weight of  $2 \times 10^{-6}$  kg at the outlet.

5.2. “DF” in Empty Test Section. To ensure that the DF dependence mentioned above was a real phenomenon of the pool scrubbing, an experiment (EW1 in Table 1) was performed to measure particle number ratio between the inlet and outlet of the test section without water, named here as DF in convenience. The experimental conditions are summarized in Table 1. Two different WELAS sensors were installed at the inlet and outlet of the test section, respectively. No dilution system was applied in this experiment. DF was derived from the measurement results of WELAS sensors. The volumetric air flow rate at the exit of the injection nozzle was the same as the previous pool scrubbing experiments.

Detailed information of aerosol measurement in this experiment is presented in Table 4. The experimental procedure was similar to the experiment PW1. The experiment started from the lowest particle number concentration and the concentration was increased by adjusting the aerosol generation system. After setting a new particle number concentration condition, a waiting time was provided. During each waiting time, particle number concentration changes at the inlet and outlet were monitored by the WELAS sensors. The monitoring time in all the number concentration conditions was in the range of 300 - 900 s. After reaching a steady-state condition, aerosol particle number distributions in particle diameter at the inlet and outlet were measured by the WELAS sensors simultaneously for obtaining DF. In each particle number concentration condition, WELAS measurements in a measurement time were repeated usually more than 3 times. A value of DF was obtained in each measurement based on (4) without substituting the dilution rate. In order to measure enough particles statistically, the measurement time was longer in lower particle number concentration and in the range of 100 - 600 s. More than  $7 \times 10^4$  particles were measured in each measurement.

In this experiment, mode diameters measured by WELAS at the inlet and outlet were  $0.5 \mu\text{m}$  in all the total particle number concentrations. All the DFs were plotted against total particle number concentrations at the outlet as shown in Figure 5. It was obvious that DF was independent of the aerosol number concentration in the empty test section.

Therefore, it was indicated that the DF dependence was a real phenomenon of the pool scrubbing. In addition, all the DFs were almost one, which confirmed that the particle loss of our experimental system was limited and ensured its ability to obtain an accurate DF in the pool scrubbing experiment.

## 6. Experimental Investigation on Characteristics of DF Dependence

To investigate characteristics of the DF dependence, pool scrubbing experiments (PW2, PW3, and PW4) were performed in other three different water submergences (0.3, 0.8, and 1.6 m) in addition to the experiment PW1 in the submergence of 2.4 m. The experimental conditions are summarized in Table 1. In all the experiments, aerosol measurement installation was the same as the experiment PW1: two different WELAS sensors at the inlet and outlet and the dilution system at the inlet only. Both WELAS sensors were heated to 393 K. The volumetric air flow rate at the exit of the injection nozzle was the same as the previous experiments. Temperatures of air and water were also close to those in the experiment PW1.

Detailed information of aerosol measurement in this experiment is presented in Table 5. The experimental procedure of these experiments was totally the same as the experiment PW1. In each experiment, particle number concentration was increased monotonically by adjusting the aerosol generation system. In each condition of particle number concentration, a waiting time was provided with monitoring particle number concentration changes at the inlet and outlet. Afterwards, aerosols at the inlet and outlet were measured simultaneously by two different WELAS sensors for several times for obtaining DF based on (4) with the dilution rate of 8.7. More detailed description of the procedure can be found in Section 4.

In these experiments, mode diameters measured by WELAS at the inlet and outlet were  $0.5 \mu\text{m}$ . The DFs and the total particle number concentrations at the inlet and outlet obtained in each particle number concentration condition were averaged based on (7)–(9), respectively. All the averaged DFs in all the water submergences were plotted against the averaged total particle number concentrations at the inlet and the outlet as shown in Figures 6(a) and 6(b), respectively.

TABLE 5: Aerosol measurement information of the experiments PW2-PW4.

Experiment	Averaged number concentration at outlet* (1/m <sup>3</sup> )	Monitoring time (s)	Measurement time (s)	Number of measurements (-)
PW2	2.9×10 <sup>8</sup>	900	900	5
	7.6×10 <sup>8</sup>	900	600	5
	2.2×10 <sup>9</sup>	600	300	6
	5.5×10 <sup>9</sup>	300	300	7
	1.7×10 <sup>10</sup>	600	300	5
	3.1×10 <sup>10</sup>	300	250	2
	4.3×10 <sup>10</sup>	600	300	8
	6.8×10 <sup>10</sup>	600	300	5
	1.1×10 <sup>11</sup>	600	300	5
PW3	8.0×10 <sup>9</sup>	600	900	4
	1.7×10 <sup>10</sup>	510	600	5
	2.6×10 <sup>10</sup>	600	300	4
	3.1×10 <sup>10</sup>	300	300	4
	6.5×10 <sup>10</sup>	300	300	5
	1.1×10 <sup>11</sup>	300	300	3
PW4	4.3×10 <sup>9</sup>	900	900	3
	6.8×10 <sup>9</sup>	900	600	5
	1.2×10 <sup>10</sup>	600	600	5
	2.6×10 <sup>10</sup>	600	300	5
	5.0×10 <sup>10</sup>	300	300	5
	6.7×10 <sup>10</sup>	360	150	2

\*Condition was set in the order from the top.

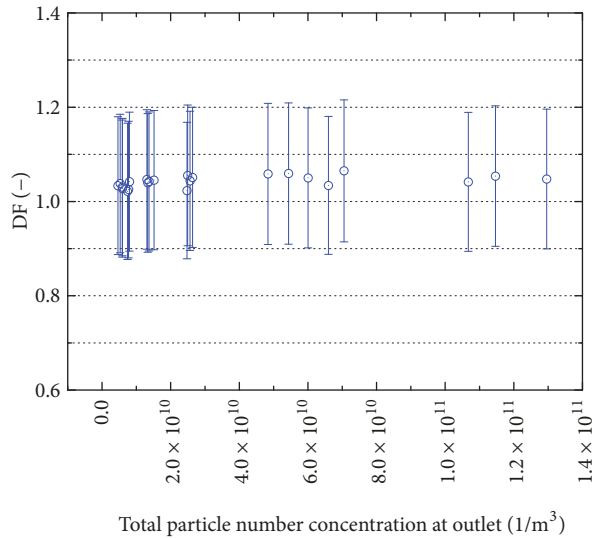


FIGURE 5: DFs in empty test section.

In all the submergences, the DF dependence on the aerosol particle number concentration was observed in the same tendency. DF increased with decreasing the concentration and tended to approach a constant value with increasing the concentration. In low water submergences of 0.3 m and 0.8 m, the DF dependences were not clear and all the DFs were

within measurement errors. With increasing water submergence, the DF dependence became more significant. In 1.6 m water submergence, an obvious DF dependence appeared in particle number concentrations lower than  $1.2 \times 10^{11} / \text{m}^3$  at the inlet taking the error of DF into consideration. Roughly speaking, the DF dependences in both 1.6 m and 2.4 m water

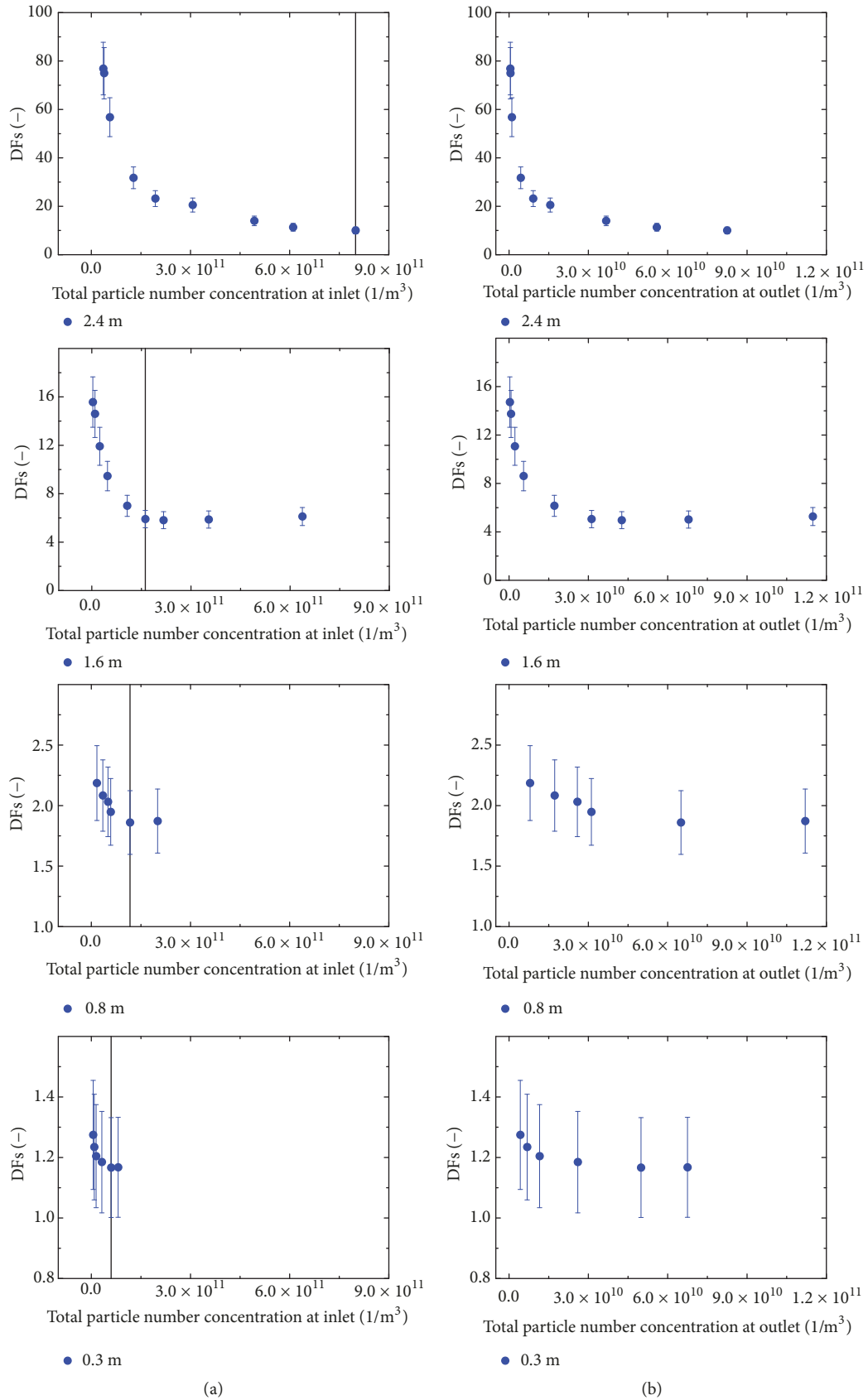


FIGURE 6: DFs in all water submergences against total particle number concentrations (a) at inlet and (b) at outlet.

submergences became significant below this concentration, although a moderate DF dependence still existed in 2.4 m water submergence beyond this concentration. According to these results, it was suggested to pay more attention to the condition with high water submergence and low particle number concentration: for example, higher than 1.6 m and lower than around  $1 \times 10^{11} / \text{m}^3$ . However, it is necessary to note that the particle number concentration with a significant DF dependence will rely on thermohydraulic conditions, particle characteristics, and so on.

In addition, the lowest inlet particle number concentration to approach a constant DF was indicated by a vertical line for each submergence in Figure 6(a). With increasing the submergence, this concentration increased monotonically. In 2.4 m water submergence, it seems that the highest concentration was even not enough to reach a constant value of DF. In other words, the lowest concentration at the inlet for a constant DF in a lower submergence was not enough to approach a constant DF in a higher submergence. This will also be an evidence to support that the DF dependence occurs in the water pool and is a real phenomenon of the pool scrubbing. For example, a total inlet particle number concentration of  $1.6 \times 10^{11} / \text{m}^3$  was enough for a constant value of DF in the submergence of 1.6 m but not enough in the submergence of 2.4 m. Assuming that the gas-liquid two-phase flow behaviors, equivalent to aerosol reduction efficiencies, from the injection nozzle exit to 1.6 m downstream are almost the same in the 1.6 m and 2.4 m submergence experiments with the same volumetric air injection flow rate, the DF dependence will result between 1.6 m and 2.4 m downstream from the nozzle exit.

## 7. Discussion about DF Dependence

To begin with, several critical assessments of the aerosol measurement and the experimental procedure for the DF dependence are discussed as follows:

(1) An experimental procedure and the time for setting up conditions may cause an error of DF. For example, when we set up conditions with increasing particle number concentration stepwise, DF may be overestimated if an aerosol measurement for DF begins immediately after changing the condition without allowing the particles to reach the outlet. In our experiments, a waiting time was always provided after changing an aerosol particle number concentration condition and the number concentration change was monitored by WELAS during the time for achieving a steady-state condition. In the empty test section, the gas velocity was 0.04 m/s in the air flow rate of  $1.3 \times 10^{-3} \text{ m}^3/\text{s}$ . Time for particles with the flow passing through the empty test section with a length of 2.4 m can be estimated to be around 60 s. In the pool scrubbing experiment with 2.4 m water submergence, the time can be shorter than 6 s taking the cross-sectional averaged bubble rising velocity of 0.5 m/s described in Section 4 into consideration. Therefore, the waiting time longer than 300 s in our experiments will be enough for particles reaching the outlet. In addition, the condition in the sampling filter experiment, for example PFI, was not set to increase particle number concentration

monotonically. The aerosol measurement for DF (=37) in the lowest concentration case was performed after the highest concentration case with a smaller value of DF. Therefore, the DF dependence will not be a result of this experimental procedure.

(2) In our experiment apparatus, there is not any filter installed between the outlet of the test section and the environment. Therefore, air velocity fluctuation and turbulent eddy may be generated at the outlet aerosol sampling location by the environment. They can affect an aerosol sampling there in general and lead to an error of DF. However, this effect was not evident or at least will not be a reason to cause the DF dependence in the pool scrubbing experiment taking the DF results in the empty test section into consideration. A constant value of DFs in the empty test section was confirmed until  $4.6 \times 10^9 / \text{m}^3$ .

(3) If WELAS has nonlinear characteristics against particle number concentration, the DF dependence on the concentration can be observed. In principle, a particle number counting error of WELAS can occur in a high particle number concentration due to multiparticles entering its sensing volume simultaneously but not in a low particle number concentration. The measurement error of particle number concentration by WELAS was confirmed by CPC in the concentration range of  $4 \times 10^9 - 1.2 \times 10^{11} / \text{m}^3$  [13] and the error was included in the error of DF. Therefore, the DF dependence was not attributed to WELAS characteristics in the conditions of the concentration higher than  $4 \times 10^9 / \text{m}^3$  which corresponded to those with DF lower than 32 in 2.4 m water submergence and with DF lower than 9 in 1.6 m. Although there are not any WELAS characteristics in a low particle number concentration in principle, more significant DF dependence in lower concentration was not validated from this viewpoint.

Next, several mechanisms to explain a DF dependence on the aerosol concentration are discussed as follows:

(1) Particle agglomeration in high particle number concentration will result in a DF dependence on the concentration. However, DF in a higher concentration should have a higher value due to more particle removal of large agglomerates. This DF tendency is different from our result. Therefore, the DF dependence we obtained is not due to this mechanism.

(2) Particle inertia may affect a gas flow if particle concentration is high enough, which may result in DF value change. The initial momentums of gas and all the test particles ( $0.5 \mu\text{m}$  spherical particles), in other words the initial masses of gas and the test particles by assuming the same initial velocity, are considered. The momentum of all the particles in the highest inlet particle number concentration of  $8 \times 10^{11} / \text{m}^3$  is calculated to be around 0.01% of that of the gas. Therefore, effect of the particle inertia on the gas flow will be limited and this mechanism will not lead to the DF dependence we obtained.

(3) More particles may be removed due to particle size growth by a water condensation on a particle surface during bubble rising, which increases DF value. After a gas injection to the pool water, initial bubbles will become saturated

to the water temperature immediately. During the bubble rising, gas temperature of bubbles will be decreasing due to a bubble expansion by a hydrostatic pressure reduction. For example, if an adiabatic expansion of an air bubble with the initial gas temperature of 280 K is assumed in a water submergence of 0.8 m, the gas temperature of the bubble reaching water surface is estimated to be about 274 K. In fact, the gas temperature decrease will be more moderate than this estimation, since the heat transfer from the water to the bubble occurs. The particle temperature can be regarded as the gas temperature lower than the water temperature because of small heat capacity of the particles with small mass. Accordingly, water condensation on the particles will occur in this supersaturated atmosphere during the bubble rising. Vapor amount in a bubble depends on thermal hydraulic condition. However, it does not depend on particle concentration. Therefore, particle growth is expected to be more remarkable in lower particle concentration for sharing the same vapor amount, which results in more particle removal in lower particle concentration. Based on this mechanism, DF will increase in lower particle concentration and the tendency of DF dependence we obtained can be explained. In order to confirm that our result is mainly caused by this mechanism, an experiment in higher water temperature and one with soluble test particles are helpful and will be our future work. In a higher water temperature, higher supersaturation and more extra vapor amount in a rising bubble are expected with the same gas temperature decrease. Therefore, the particle growth will be more remarkable in such atmosphere. On the other hand, the material of soluble particles will be dissolved in a saturated atmosphere and a solution will be formed on the particle surface. The equilibrium vapor pressure above the solution is lower than that above a pure water, which allows a stable water condensation on a soluble particle surface even in a saturated or unsaturated atmosphere. Therefore, the particle growth of soluble particles will be more remarkable than the insoluble SiO<sub>2</sub> particles. More significant DF dependence is expected to be observed in both experiments due to this mechanism.

(4) Contamination on bubble surface will affect the bubble motion and the internal gas circulation flow in a bubble, which will change DF value. In the pool scrubbing process, before hydrophilic SiO<sub>2</sub> particles transport from gas in a bubble to the water completely, they must adhere on the bubble surface once. Accordingly, the bubble surface will be contaminated to some extent by the particles. Compared to a bubble with clean surface, slip between gas and liquid on a contaminated bubble surface can be reduced [18, 19]. Accordingly, highly contaminated bubble in higher aerosol concentration will have lower internal gas circulation velocity due to weaker slip, which reduces particle removal by centrifugal deposition in the bubble and decreases DF value. Based on this mechanism, DF will decrease with increasing aerosol concentration and the tendency of DF dependence we obtained can be explained. In order to investigate this mechanism, an experiment by using hydrophobic test particles is helpful and will be our future work. Particle detachment from a bubble surface to the water for hydrophobic particles will be limited compared with hydrophilic particles. Consequently,

the bubble surface will be more contaminated and more significant DF dependence is expected to be observed with hydrophobic particles.

## 8. Conclusion

Because a pool scrubbing is very important to reduce radioactive aerosols to the environment for a nuclear reactor in a severe accident situation, many researches have been performed. In these researches, DF dependence on the aerosol concentration was seldom considered in an aerosol concentration with limited aerosol coagulation.

In this paper, DF dependence on aerosol particle number concentration in the pool scrubbing with 2.4 m water submergence was measured. It was observed that DF increased monotonically with decreasing the concentration in the constant thermohydraulic condition: a gradual increase from 10 to 32 in the range of  $1.3 \times 10^{11}$  -  $8.0 \times 10^{11}/\text{m}^3$  at the inlet and a significant increase from 32 to 77 in the range of  $3.6 \times 10^{10}$  -  $1.3 \times 10^{11}/\text{m}^3$ . By two validation experiments, we confirmed that the moderate DF dependence, DF from 10 to 32, was not due to measurement errors and might be a real pool scrubbing phenomenon. Subsequently, characteristics of the DF dependence were investigated experimentally by measuring the DF dependence in other three different water submergences. The experimental results indicated that the DF dependence resulted from a certain distance in the downstream of the gas injection nozzle to the water surface. In addition, it was found that the DF dependence was more significant in higher water submergence. Roughly speaking, a significant DF dependence was observed in the condition of water submergence higher than 1.6 m and inlet particle number concentration less than around  $1 \times 10^{11}/\text{m}^3$  in our experiments. It is recommended to perform further analysis for the DF dependence mainly in such condition, since the observed DF dependence is usually not accounted for and could make a difference to both experiment and model of the pool scrubbing. Several possible mechanisms to explain the DF dependence were discussed, including phenomena of condensation on particle surface and contamination on bubble surface. They will be investigated by our future experiments described in Section 7 for each phenomenon to ensure main reasons for the DF dependence.

## Data Availability

All data included in this study are available upon request by contacting the corresponding author.

## Conflicts of Interest

The authors declare that there are no conflicts of interest regarding the publication of this paper.

## Acknowledgments

This experimental system, especially aerosol instrumentation was developed under the auspices and financial support of the Nuclear Regulation Authority (NRA), Japan.

## References

- [1] P. Owczarski and K. Burk, "SPARC-90: A code for calculating fission product capture in suppression pools," Tech. Rep. NUREG/CR-5765, 1991.
- [2] S. A. Ramsdale, "BUSCA-JUN90 referenbece nabyak, SRD-R542," 1991.
- [3] A. T. Wassel, A. F. Mills, D. C. Bugby, and R. N. Oehlberg, "Analysis of radionuclide retention in water pools," *Nuclear Engineering and Design*, vol. 90, no. 1, pp. 87–104, 1985.
- [4] I. Kaneko, M. Fukasawa, M. Naito, K. Miyata, and M. Matsumoto, "Experimental study on aerosol removal effect by pool scrubbing," in *Proceedings of the 22nd DOE/NRC Nuclear Air Cleaning and Treatment Conference*, pp. 24–27, August 1992.
- [5] B. M. Escudero, C. M. J. Marcos, K. M. Swiderska, E. M. Martin, and J. J. Lopez, *State-of-the-Art Review on Fission Products Aerosol Pool Scrubbing under Severe Accident Conditions*, Nuclear science and technology, 1995.
- [6] L. E. Herranz, V. Peyrés, J. Polo, M. J. Escudero, M. M. Espigares, and J. López-Jiménez, "Experimental and analytical study on pool scrubbing under jet injection regime," *Nuclear Technology*, vol. 120, no. 2, pp. 95–109, 1997.
- [7] A. Dehbi, D. Suckow, and S. Guentay, "Aerosol retention in low-subcooling pools under realistic accident conditions," *Nuclear Engineering and Design*, vol. 203, no. 2-3, pp. 229–241, 2001.
- [8] S. Uchida, A. Itoh, M. Naitoh et al., "Temperature dependent fission product removal efficiency due to pool scrubbing," *Nuclear Engineering and Design*, vol. 298, pp. 201–207, 2016.
- [9] T. Kanai, M. Furuya, T. Arai, and Y. Nishi, "Development of an aerosol decontamination factor evaluation method using an aerosol spectrometer," *Nuclear Engineering and Design*, vol. 303, pp. 58–67, 2016.
- [10] K. Hashimoto, K. Soda, S. Uno, H. Nakatani, and H. Takeoka, "Effect on pool scrubbing of insoluble aerosol in two phase flow in a pipe," *Severe Accidents in Nuclear Power Plants*, vol. 2, pp. 77–86, 1988.
- [11] H. J. Allelein, A. Auvinen, J. Ball et al., "State-of-the-art report on nuclear aerosols," NEA/CSNI/R(2009)5, 2009.
- [12] B. Clément, N. Hanniet-Girault, G. Repetto et al., "LWR severe accident simulation: Synthesis of the results and interpretation of the first Phebus FP experiment FPT0," *Nuclear Engineering and Design*, vol. 226, no. 1, pp. 5–82, 2003.
- [13] H. Sun, S. Machida, Y. Sibamoto, Y. Okagaki, and T. Yonomoto, "Experimental investigation on dependence of decontamination factor on aerosol number concentration in pool scrubbing under normal temperature and pressure," in *Proceedings of the 2018 26th International Conference on Nuclear Engineering*, London, UK, 2018.
- [14] K. Pramod, A. B. Paul, and W. Klaus, *Aerosol Measurement: Principles, Techniques, and Applications*, John Wiley & Sons, 2011.
- [15] H. Sun, Y. Sibamoto, Y. Okagaki, and T. Yonomoto, "Development of error reduction methods in aerosol measurement for pool scrubbing experiment," in *Proceedings of the 2016 24th International Conference on Nuclear Engineering, ICONE 2016*, Charlotte, NC, USA, June 2016.
- [16] Y. T. Shah, B. G. Kelkar, S. P. Godbole, and W. D. Deckwer, "Design parameters estimations for bubble column reactors," *AIChE Journal*, vol. 28, no. 3, pp. 353–379, 1982.
- [17] K. Akita and F. Yoshida, "Bubble size, interfacial area, and liquid-phase mass transfer coefficient in bubble columns," *Industrial & Engineering Chemistry Process Design and Development*, vol. 13, no. 1, pp. 84–91, 1974.
- [18] M. Rastello, J.-L. Marie, and M. Lance, "Clean versus contaminated bubbles in a solid-body rotating flow," *Journal of Fluid Mechanics*, vol. 831, pp. 592–617, 2017.
- [19] R. Clift, J. R. Grace, and M. E. Weber, *Bubbles, Drops, and Particles*, Dover edition, 1978.

